Evaluating the potential of a solid dispersion of curcumin in the management of osteoarthritis

Onwunedo Afomachukwu Chinelo*[1], Modozie Benjamin Uchenna[2], Uronnachi Emmanuel[1]

[1]Department of Pharmaceutics and Pharmaceutical Technology, Faculty of Pharmaceutical Sciences, Nnamdi Azikiwe University, Agulu, Anambra State, Nigeria

[2]Department of Pharmaceutical and Medicinal Chemistry, Faculty of Pharmaceutical Sciences, Nnamdi Azikiwe University, Agulu, Anambra State, Nigeria

Submitted: 5th August, 2026; Accepted: 20th Oct., 2026; Published online: 31st Oct., 2026
DOI: https://doi.org/10.54117/jcbr.v6i5.2
**Corresponding Author: Afomachukwu Onwunedo; afomachukwu2015@gmail.com*

Abstract

Osteoarthritis (OA) is a progressive degenerative joint disorder characterized by cartilage breakdown, swelling, pain, and functional impairment. Pharmacotherapy provides symptomatic relief limited by adverse effects during long-term use. Curcumin exhibits anti-inflammatory and antioxidant properties relevant to OA management but has poor oral bioavailability. This study was aimed at formulating and characterizing solid dispersions of curcumin using sodium starch glycolate (SSG) as the hydrophilic carrier, while assessing its therapeutic efficacy on osteoarthritis. The solvent evaporation method was used to prepare solid dispersions of curcumin (SDC) at different ratios of 1:1 (Batch A), 1:2 (Batch B) and 2:1 (Batch C) of curcumin to SSG respectively. The SDCs were evaluated for percentage loading, aqueous solubility, flow characteristics, differential scanning calorimetry (DSC) and Fourier transform infrared spectroscopy (FTIR). Stability was also evaluated. The *in-vivo* anti-inflammatory effect was investigated using albino rats while limping behaviour, knee swelling and percentage arthritic inhibition were assessed. The batch B SDC exhibited the best *in vitro* release and had a 2.4-fold increase in solubility relative to batch A. DSC thermograms showed reduction in curcumin crystallinity for all batches. FTIR did not show any chemical interaction between curcumin and SSG. Batch B exhibited fair flow with compressibility index of 17 % and Hausner's quotient of 1.2. Batch B showed the least degradation during stability testing after 4 weeks. Batch B achieved the highest reduction in limping and swelling, closely approximating diclofenac group which served as the positive control. Percentage arthritic inhibition increased over 28 days, with batch B showing superior efficacy compared to other formulations.

Keywords: Solid dispersions; curcumin; osteoarthritis; monoiodoacetate; dissolution.

For abstracting and indexing purposes: **Curcumin solid dispersion for Arthritis**

Introduction

Osteoarthritis (OA) is one of the leading causes of disability worldwide, particularly among the aging population. Current therapeutic strategies for osteoarthritis are primarily palliative, focusing on symptomatic relief through the use of non-steroidal anti-inflammatory drugs (NSAIDS), corticosteroids, and physical therapy. However, these approaches are often associated with significant side effects, limited long-term efficacy, and do not address the underlying disease progression (Pari *et al*, 2008). These setbacks have led scientists into exploring nutraceuticals as possible alternatives for managing OA and to decrease the disease progression.

Curcumin, a polyphenolic compound derived from *Curcuma longa*, has garnered significant interest due to its potent anti-inflammatory, antioxidant, and chondroprotective properties (Aggarwal and Harikumar, 2009). It has applications in various disease conditions such as type 2 diabetes mellitus (Meng *et al.*, 2013), cardiovascular disease (Hernandez *et al.,*2016), fatty liver disease (Nabavi *et al*., 2014) and cancer (Liu *et al*., 2018). Despite its therapeutic potential, the clinical application of curcumin in OA management remains limited due to its poor aqueous solubility, low oral bioavailability, and rapid systemic elimination (Fu *et al*, 2016). Over the years, formulation experts have employed several methods such as solid dispersion (SD) (Xu *et al*., 2018); complexation (Mohammadia *et al.*, 2019); lipid-based systems (Chen *et al*., 2018); micronization (Seo *et al*., 2016); nanonization (Wong *et al*., 2018); and co-crystallization (Reggane *et al.*, 2018) to improve the solubility and bioavailability of poorly water-soluble drugs like curcumin. Among these the solid dispersion method is one of the most successful methods.

In this investigation, the solid dispersion technique was employed to boost the solubility, stability and systemic absorption of curcumin by dispersing it in a suitable carrier matrix, potentially improving its therapeutic outcomes in osteoarthritic patients (Choi *et al*, 2018). Sodium starch glycolate was used as a suitable hydrophilic carrier due to its safety, minimum cost, chemical compatibility, greater aqueous solubility, ability to generate solid dispersion in an amorphous form and enhancement of significant drug absorption (Verheyen *et al*., 2002; Franco *et al*., 2001; Shihora and Panda, 2011). Therefore, this study was aimed at increasing curcumin's dissolution rate and aqueous solubility by dispersing it in sodium starch glycolate using the solvent evaporation method, and evaluating its anti-arthritic effect in an animal model.

Materials and methods

Materials

Curcumin was bought as a drug sample from ChromaDex (USA). Sodium starch glycolate was purchased from Merck & Co., Inc. (Germany), monoiodoacetate, 2% lidocaine, Formaldehye 40 % (CIL chemicals, Nigeria), ethanol, acetone, diethylaether, ethyl acetate

(Guangdong Guanghua Sci-Tech Co. Ltd., China) were used. The membrane filter (0.2 μm) was used to filter analyte samples. The chemicals and solvents used in the laboratory were of analytical grade.

Methods

Preparation of curcumin solid dispersion (SDCs)

Using various weight ratios of drug and carrier (w/w) (Table 1), the solid dispersions of curcumin were formulated using the solvent evaporation method (Yu *et al,* 2020). The desired proportions of curcumin powder and sodium starch glycolate were dissolved in 100 ml of ethanol in a 200 ml flask according to the formula in table 1. A magnetic stirrer was used to stir the solution continuously at a speed of 100 rpm at 50 °C in order to evaporate the solvent from the dispersion system. The remaining solid dispersion was dried at room temperature following the complete solvent evaporation before being ground into a fine powder. Finally, the dried SDCs were passed through a 120-mesh screen to get dried granules of uniform size. Three SDC batches were prepared. The preparations were kept at room temperature in a screw-cap vial for further evaluations.

Table 1- Preparation of curcumin solid dispersion (SDC)

Batch	Ratio of curcumin to sodium starch glycolate	Quantity of Curcumin (mg)	Quantity of Sodium starch glycolate (mg)
A	1:1	150	150
B	1:2	150	300
C	2:1	300	150

Micromeritic Properties of the powders

Carr's compressibility index:

A 100 g quantity of curcumin solid dispersion was weighed and poured into a graduated cylinder and the volume of powder noted as bulk volume. The bulk density was calculated using the formula

$$\text{Bulk density} = \frac{\text{mass}}{\text{bulk volume}} \quad \ldots\ldots\ldots\ldots\ldots\ldots\ldots\ldots\ 1$$

Afterwards, the powder was tapped 100 times manually and the volume of powder was noted as tapped volume and the tapped density was calculated using the formula

$$\text{Tapped density} = \frac{\text{mass}}{\text{tapped volume}} \quad \ldots\ldots\ldots\ldots\ldots\ldots\ldots\ldots\ldots\ldots\ 2$$

The steps above were repeated 5 times and the average used to calculate Carr's index with the formula:

$$\text{Carr's index} = \frac{(\text{tapped density} - \text{bulk density})}{\text{tapped density}} \quad \ldots\ldots\ldots\ldots\ldots\ 3$$

Hausner's Quotient

This was calculated using the formula:

$$\text{Hausner ratio} = \frac{\text{Tapped density}}{\text{Bulk Density}} \quad \ldots\ldots\ldots\ldots\ldots\ldots\ldots\ 4$$

Preparation of stock solution

A stock solution containing 100 µg/ml of curcumin was prepared. A 10 mg quantity of curcumin was accurately weighed and transferred into a 100 ml volumetric flask and made up to the mark with ethylacetate. Serial dilutions of the solution using ethylacetate were prepared to obtain concentrations of 1-5 µg /ml.

Preparation of standard calibration curve

The wavelength of maximum absorption (λ_{max}) was determined by scanning a 100 µg/ml solution of curcumin using UV-Visible double beam spectrophotometer [Searchtech Spectrometer, model 750N, China] from 400-500 nm using ethylacetate as blank. Afterwards, the absorbance of the stock solutions in ethyl acetate at 1-5 µg/ml were measured at 420 nm. Standard calibration curve was prepared by plotting average (n=3) absorbance versus concentration.

Estimation of curcumin in the solid dispersions

A stock solution (100 µg/ml) was prepared by dissolving 10 mg of powder from each batch of solid dispersion in 100 ml volumetric flask using ethyl acetate. The solution was sonicated for 15 mins and filtered through membrane filter (0.2 µm). Afterwards, a test solution of 5 µg/ml was obtained by dilution of the filtered stock solution. With ethyl acetate.

The percentage of curcumin present in the test solution of the different batches of solid dispersion was estimated using spectroscopic method. Maximum absorbance was measured at 420 nm against ethyl acetate as blank. The percentage drug content was calculated using the following formula:

$$\text{Percentage (\%) drug content: } \frac{\text{amount of curcumin recovered(mg)}}{\text{weight of solid dispersion sample(mg)}} \times 100 \quad \ldots\ldots\ldots\ldots\ldots 5$$

Amount of curcumin recovered: measured concentration × final volume × dilution factor.

Aqueous solubility study

An excess amount of curcumin and the different batch samples of the solid dispersion was added to 10ml of distilled water in a volumetric flask at a steady temperature of 37 °C for 24 h with intermittent shaking at 30 min intervals. Subsequently, the dispersion was filtered through a Millipore membrane filter, diluted 10- fold, and UV absorbance was measured at 420 nm.

Stability testing for the solid dispersion

About 200 mg quantities solid dispersion powders from different batches were added to the evaporating plate and then stored in an oven at 40 °C for one month, to determine the stability of the solid dispersion. The concentration of curcumin in the solid dispersion was measured every 7 days by preparing a test solution of 5µg/ml from each batch and obtaining the absorbance which was then fitted to the calibration curve. Percentage reduction was calculated for each week using the formula;

$$\text{Percentage reduction (\%)} = \frac{\text{initial value} - \text{final value}}{\text{initial value}} \times 100;$$ (Lukulay and Hokanson, 2005) ……. 7

Characterization of prepared SDCs

Fourier Transform Infrared Spectroscopy (FTIR)

A 1 g quantity of the sample was weighed using analytical weighing balance and transferred to the mortar. Afterwards, 1 g of potassium bromide (KBr) was added, grinded and homogenized. Then, 5 ml of nujol oil was mixed with the mixture in the mortar to give a paste-like mixture. The paste-like sample was loaded on the sample compartment and placed on the sample holder in the machine to allow IR radiation to pass through the sample for interaction with the sample, and the peak absorbance against wavelength was detected and displayed on a computer system connected to the FTIR spectrometer (Bulk scientific, model 530). This procedure was followed for all the samples (Curcumin, Sodium starch glycolate, batch A, batch B, and batch C).

Differential Scanning Calorimetry (DSC)

A 3 mg sample of pure curcumin, sodium starch glycolate and the various formulated batches respectively was placed in a sealed aluminium pan and analyzed from 20 to 400 °C under nitrogen flow at a rate of 10 °C per minute using a Mettler Toledo DSC machine.

Formulation of SDC capsules

A 300 mg quantity of SDC powder from a batch was weighed and poured into an empty capsule shell that was previously weighed and the result recorded. This was done for 25 capsules for the different batches.

***In vitro* dissolution study of capsules**

Using an *in vitro* dissolution test, the performance of SDC capsules from the batches were observed and they were done following the paddle method (USP Apparatus 2) by a dissolution tester (Electrolab, India), where phosphate buffer solution at pH 6.8 was used as the medium. A capsule from each batch was added to the phosphate buffer of 900 ml and it was maintained thermostatically at 37 ± 0.5 °C at 100 rpm (paddle speed). 4 ml specimens were withdrawn from the dissolution vessel at specific time intervals of 1, 2, 3, 4, 5, 6 hours and then filtered. The vessel was refilled with 4 ml of phosphate buffer solution to maintain the volume of dissolution medium. The 4 ml of filtered solution was diluted to 10 ml of distilled water in a volumetric flask. Drug content of curcumin at each point was assayed by measuring absorbance at 420 nm with the help of a UV-spectrophotometer (Shimadzu UV-1800, Japan). Three replicates of each measurement were carried out and the mean value was calculated to obtain the dissolution profile.

***In vivo* evaluation of SDCs**

A total of 30 albino rats (weighing 100-150 g) were obtained from the Animal Facility of the Department of Veterinary Physiology and Pharmacology, University of Nigeria, Nsukka. The animals were transferred to the animal house of the Department of Pharmacology and Toxicology, Nnamdi Azikiwe University where they were used for the experiment. They were housed in clean metal cages in groups of five (5), supplied potable water and fed with growers' chicken pellet feed (Guinea Feed, Nigeria). Ethical approval was obtained from the Animal research ethics committee of Nnamdi Azikiwe University, Awka.

Monoiodoacetate (MIA) - Induced OA

Osteoarthritis was induced in rats by intra-articular administration of MIA following a previously published method with appropriate modifications (Pitcher *et al*, 2016). Briefly, a single intra-articular injection containing 1 mg of MIA in 50 µL of solution was administered into each knee joint through the infrapetellar region. The MIA was dissolved in physiological saline. Local anaesthesia was provided using 2 % lidocaine before the injection procedure. Treatment with distilled water (negative control group), diclofenac (positive control group) and test formulations commenced one day after MIA induction and continued for the designated experimental period of 28 days. The extent of limping and swelling were the parameters used to determine the degree of inflammation and arthritic condition in the animals.

Inhibition percentage was calculated using the following formula:

$$\text{Percentage inhibition} = 100 \times \frac{\text{mean constrictions in control group} - \text{number of constrictions in treated group}}{\text{mean constrictons in control group}}$$

…….. 8

Treatment Procedure

The rats were randomly divided into five groups of six rats in each group. Group 1 received distilled water orally (negative control group), group 2 received 50 mg/kg of diclofenac (positive control), group 3 received 50 mg/kg of batch B, group 4 received 50 mg/kg of batch A, group 5 receive 50 mg/kg of batch C (Nicoliche *et al*.2022).

Administration of the treatment started a day post MIA induction. On the last day of the treatment duration, two (2) animals from each group were euthanized by CO_2 asphyxiation and soft tissues were removed from the medial and lateral joint capsule of contralateral saline treated femorotibial joints. Tissue samples were prepared for light microscopy using standard procedures. (Guzman *et al.,* 2003). Briefly, samples were fixed in 10 % phosphate-buffered formalin and subsequently decalcified in 5 % formic acid for 72 hours. Frontal sections of femorotibial joints were routinely processed to H&E (Hematoxylin and Eosin) slides and examined under the light microscope. All experimental procedures were conducted in accordance with the applicable institutional guidelines for care amd use of laboratory animals and were approved by the Animal research ethics committee of Nnamdi Azikiwe University, Awka under approval number NAU/AREC/2025/0184

Statistical analysis

The results obtained were presented as mean ± standard deviation (SD) using Microsoft excel 2021 and GraphPad Prism version 8 for graphical presentation.

Results

The Compressibility indices of the formulated curcumin solid dispersions (Table 2) showed that Batches A and B had Carr's Index values within the range of 15-22 %, indicating acceptable flow characteristics. Batch C exhibited a Carr's index value greater than 22 %, suggesting poorer flowability relative to the other batches.

Table 2: Carr's index of batches

Batch	Carr's Index %
A	17.19
B	18.12
C	29.17

Key: Batch A (1:1 of curcumin to SSG); Batch B (1:2 of curcumin to SSG); Batch C (2:1 of curcumin to SSG)

The results of the Hausner's quotient (Table 3) shows that Batches A and B had values of 1.208 and 1.222, respectively, suggesting moderate flow characteristics. In contrast, Batch C exhibited a markedly higher Hausner's quotient value of 1.412, placing it within the "very poor" flow category.

Table 3: Hausner's quotient for the different batch ratios

Batch	Hausner ratio
A	1.208
B	1.222
C	1.412

Key: Batch A (1:1 of curcumin to SSG); Batch B (1:2 of curcumin to SSG); Batch C (2:1 of curcumin to SSG)

Percentage curcumin content of the different batch ratios of SDC

The percentage drug content of the curcumin solid dispersions varied notably among the three batches. Batch C exhibited the highest drug content, 63.59 %, followed by batch A, 44.79 %, while the batch B displayed the lowest content, 32.99 %. This pattern indicated that the batches differed markedly in proportion of curcumin recovered during analysis.

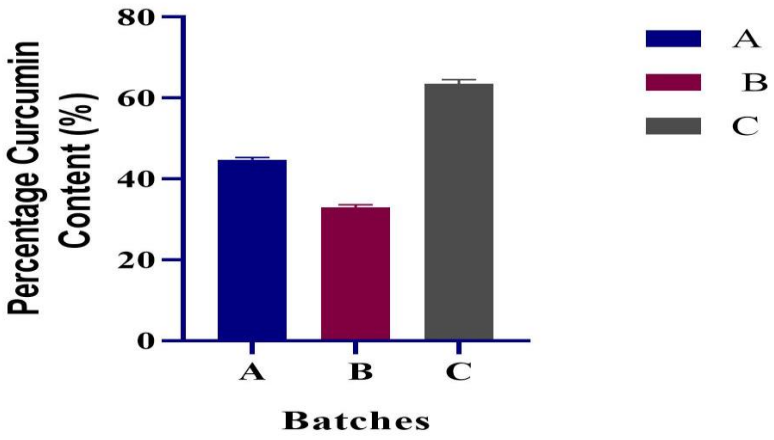

Figure 1: Percentage curcumin content in the different batches of SDC
Key: Batch A (1:1 of curcumin to SSG); Batch B (1:2 of curcumin to SSG); Batch C (2:1 of curcumin to SSG)

Aqueous solubility of the different ratios of SDC
The aqueous solubility of curcumin was evaluated for the three solid dispersion batches containing different drug: polymer ratios (1:1, 1:2, and 2:1). All solid dispersion batches showed markedly higher aqueous solubility than pure curcumin (Figure 2).
Both Batch B and Batch C exhibited significantly enhanced solubility compared to Batch A and the pure drug. Batch B, which contained a highest proportion of polymer, demonstrated approximately a 2.4-fold increase in solubility relative to Batch A.

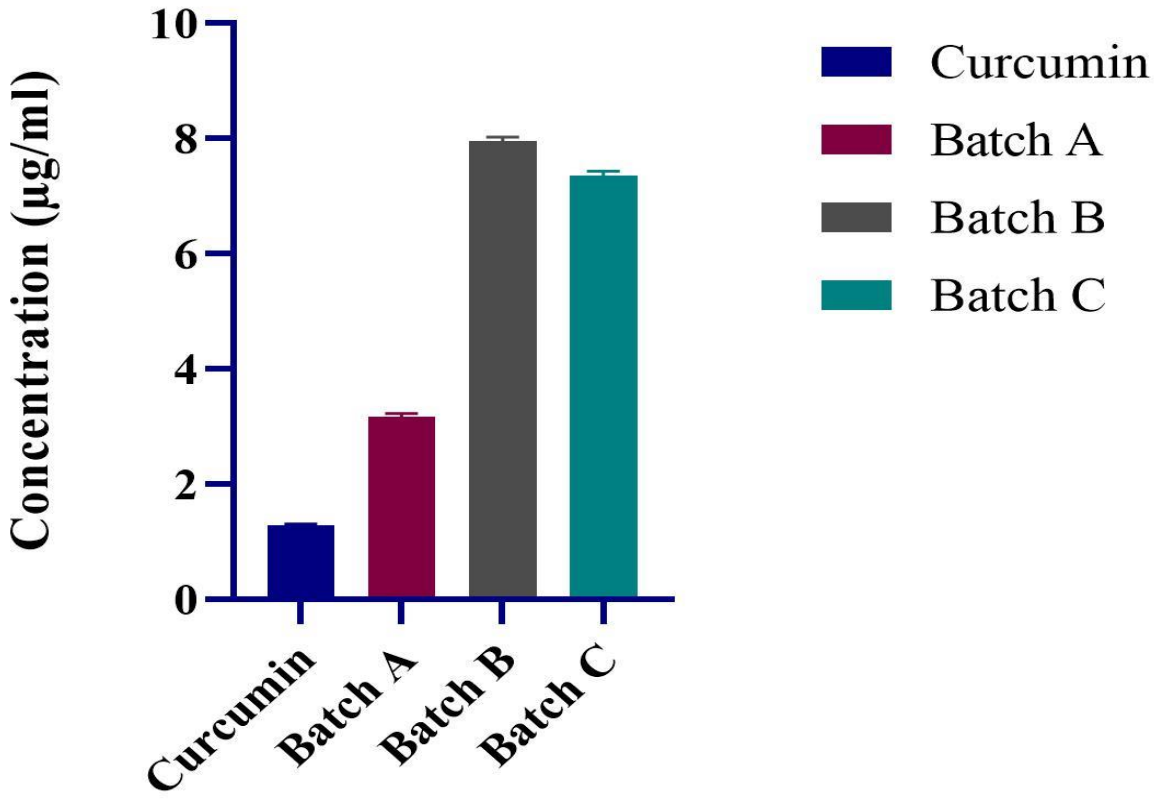

Figure 2: Aqueous Solubility of the different batch ratios of SDC
Batch A (1:1 of curcumin to SSG); Batch B (1:2 of curcumin to SSG); Batch C (2:1 of curcumin to SSG)

Fourier Transform InfraRed Spectroscopy

The FTIR spectrum of curcumin exhibited characteristic absorption bands at approximately 3500 cm^{-1}, at 3000 cm^{-1}, 1600 cm^{-1}, 1281-1243 cm^{-1} which were assigned to O-H stretching, aromatic and aliphatic C-H stretching, aromatic C=C stretching and C-O stretching vibrations, respectively. These bands were consistent with the characteristic functional groups present in curcumin.

The FTIR spectrum of sodium starch glycolate displayed a broad absorption band around 3416 cm^{-1} attributable to O-H stretching vibrations and a distinct peak at approximately 2923 cm^{-1}, corresponding to C-H stretching vibrations. Bands in the region of 1604-1400 cm^{-1} were assigned to vibrations associated with carboxylate groups, while absorptions between 1200-1000 cm^{-1} were attributed primarily to C-O-C and C-O stretching vibrations characteristic of polysaccharides. Additional bands were observed in the fingerprint region below 1000 cm^{-1}.

The FTIR spectra of the different batches of curcumin solid dispersion batches A, B, and C retained absorption bands within the aromatic stretching region of 1420-1510 cm^{-1}, together with bands attributable to O-H, C-H, and C-O vibrations. Some differences in band position, width, and intensity were observed among the formulations. These spectral variations may reflect differences in the local chemical environment of the functional groups following incorporation of curcumin into SSG matrix.

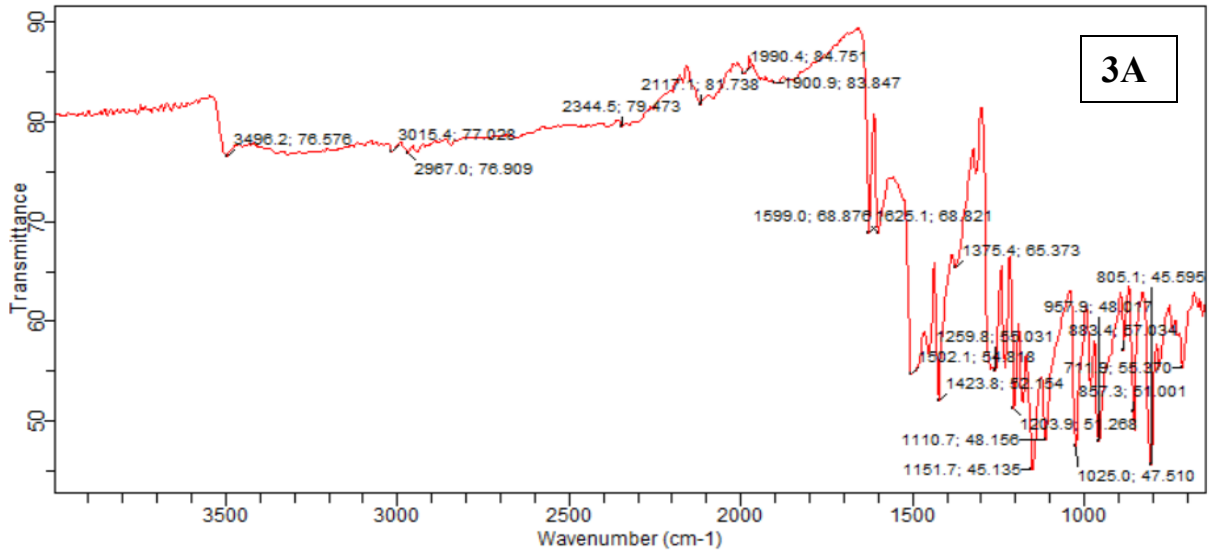

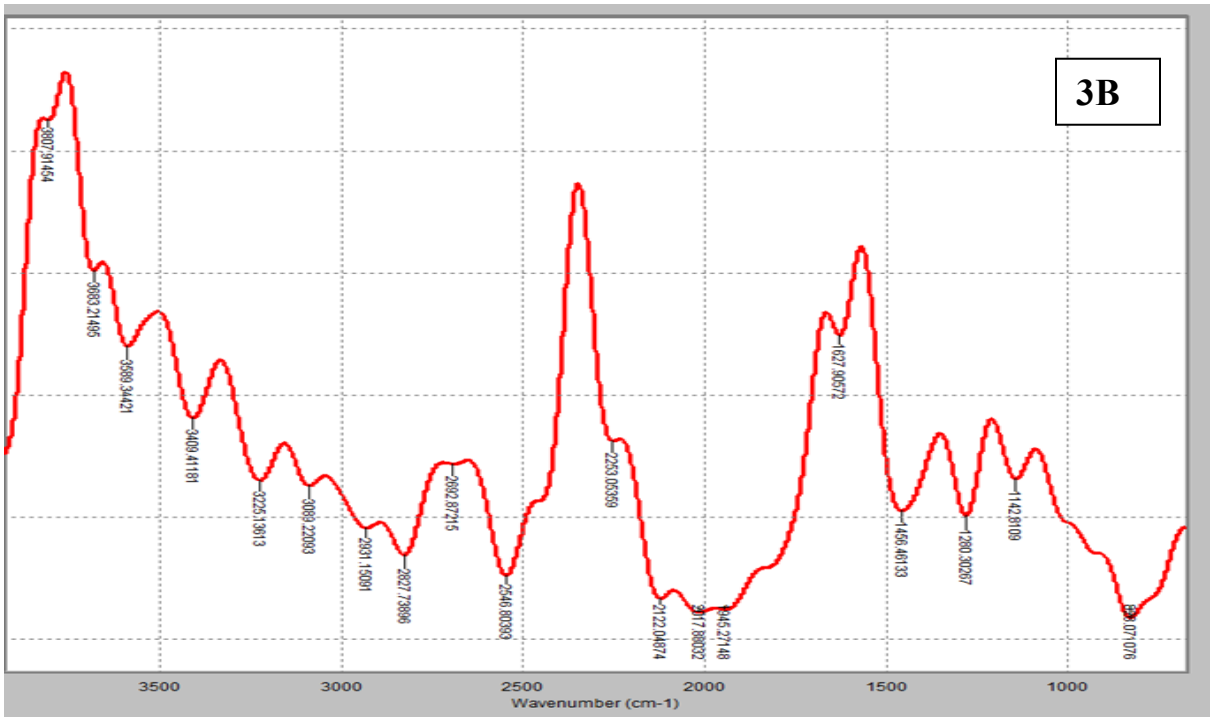
3B
3807.91454
3383.21495
3599.34421
3409.41181
3226.13613
3069.22093
2931.15091
2827.73686
2602.87215
2546.80393
2253.05389
2122.04874
2017.88032
1945.27148
1627.90572
1456.46133
1280.30267
1142.8109
1007.1076
3500
3000
2500
2000
1500
1000
Wavenumber (cm-1)

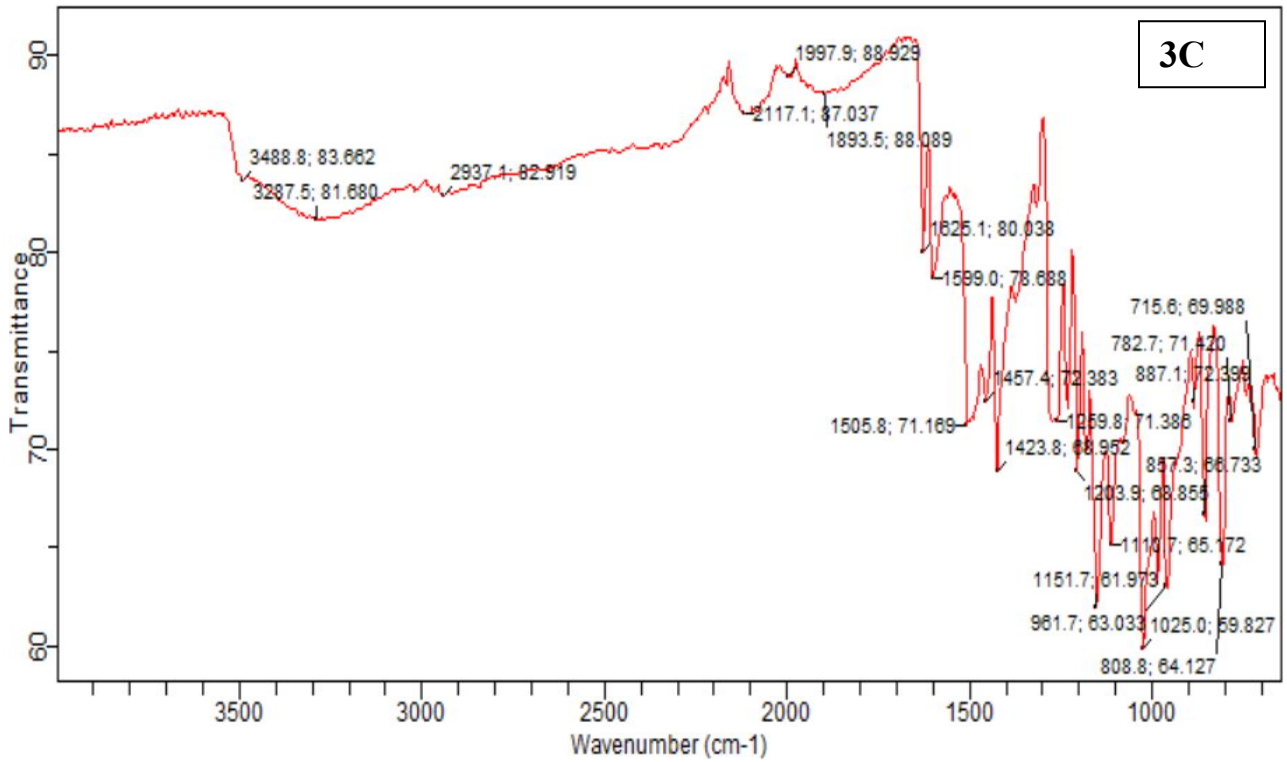
3C
1997.9; 88.929
2117.1; 87.037
1893.5; 88.089
3488.8; 83.662
3287.5; 81.680
2937.1; 82.919
1825.1; 80.038
1599.0; 78.688
715.6; 69.988
782.7; 71.420
1457.4; 72.383
887.1; 72.398
1505.8; 71.169
1259.8; 71.388
1423.8; 68.952
857.3; 66.733
1203.9; 68.855
1110.7; 65.172
1151.7; 61.973
961.7; 63.033
1025.0; 69.827
808.8; 64.127
Transmittance
90
80
70
60
3500
3000
2500
2000
1500
1000
Wavenumber (cm-1)

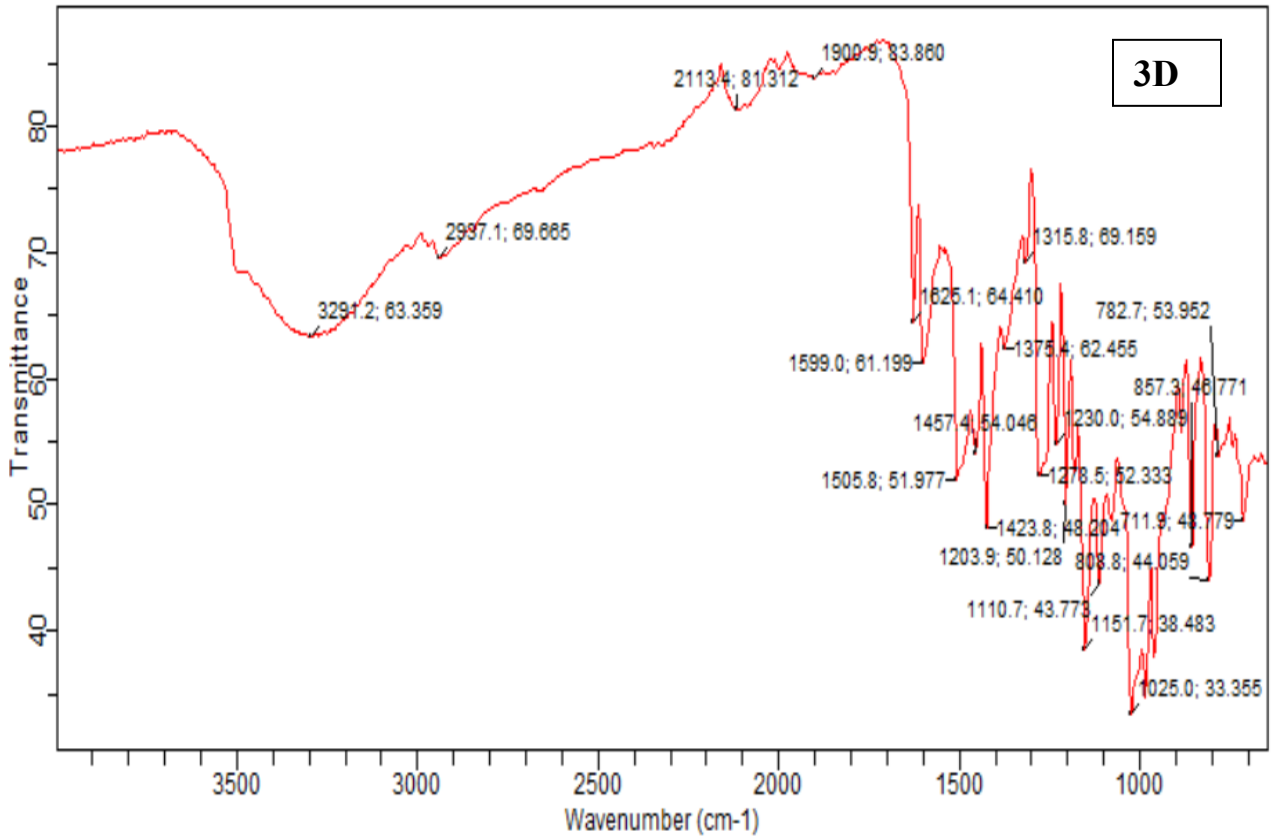
3D
Transmittance
Wavenumber (cm-1)
3291.2; 63.359
2937.1; 69.665
2113.4; 81.312
1900.9; 83.860
1625.1; 64.410
1599.0; 61.199
1505.8; 51.977
1457.4; 54.046
1423.8; 48.204
1315.8; 69.159
1375.4; 62.455
1278.5; 52.333
1230.0; 54.889
1203.9; 50.128
1151.7; 38.483
1110.7; 43.773
1025.0; 33.355
857.3; 46.771
808.8; 44.059
782.7; 53.952
711.9; 43.779

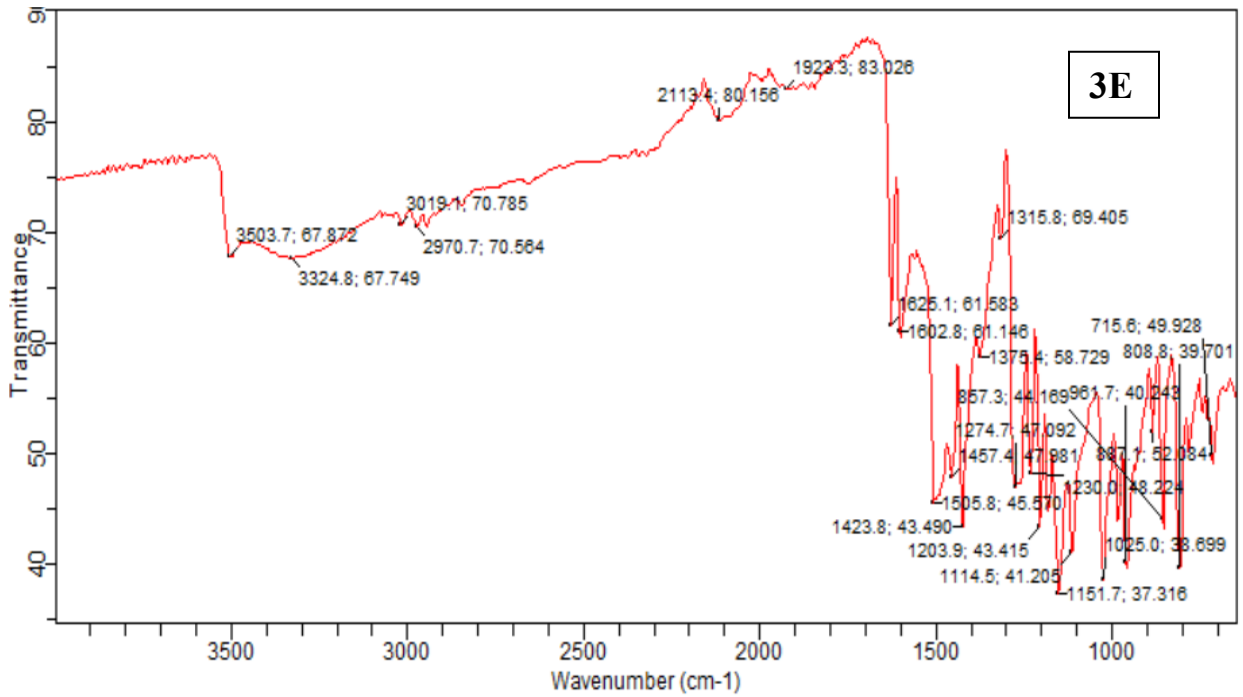
3E
Transmittance
Wavenumber (cm-1)
3503.7; 67.872
3324.8; 67.749
3019.1; 70.785
2970.7; 70.564
2113.4; 80.156
1923.3; 83.026
1625.1; 61.583
1602.8; 61.146
1505.8; 45.570
1457.4; 47.981
1423.8; 43.490
1375.4; 58.729
1315.8; 69.405
1274.7; 47.092
1230.0; 48.224
1203.9; 43.415
1151.7; 37.316
1114.5; 41.205
1025.0; 38.699
961.7; 40.243
857.3; 44.169
808.8; 39.701
715.6; 49.928

Figure 3: FTIR spectra of curcumin(3A), Sodium starch glycolate (3B), batch A (3C), batch B (3D) and batch C (3E).

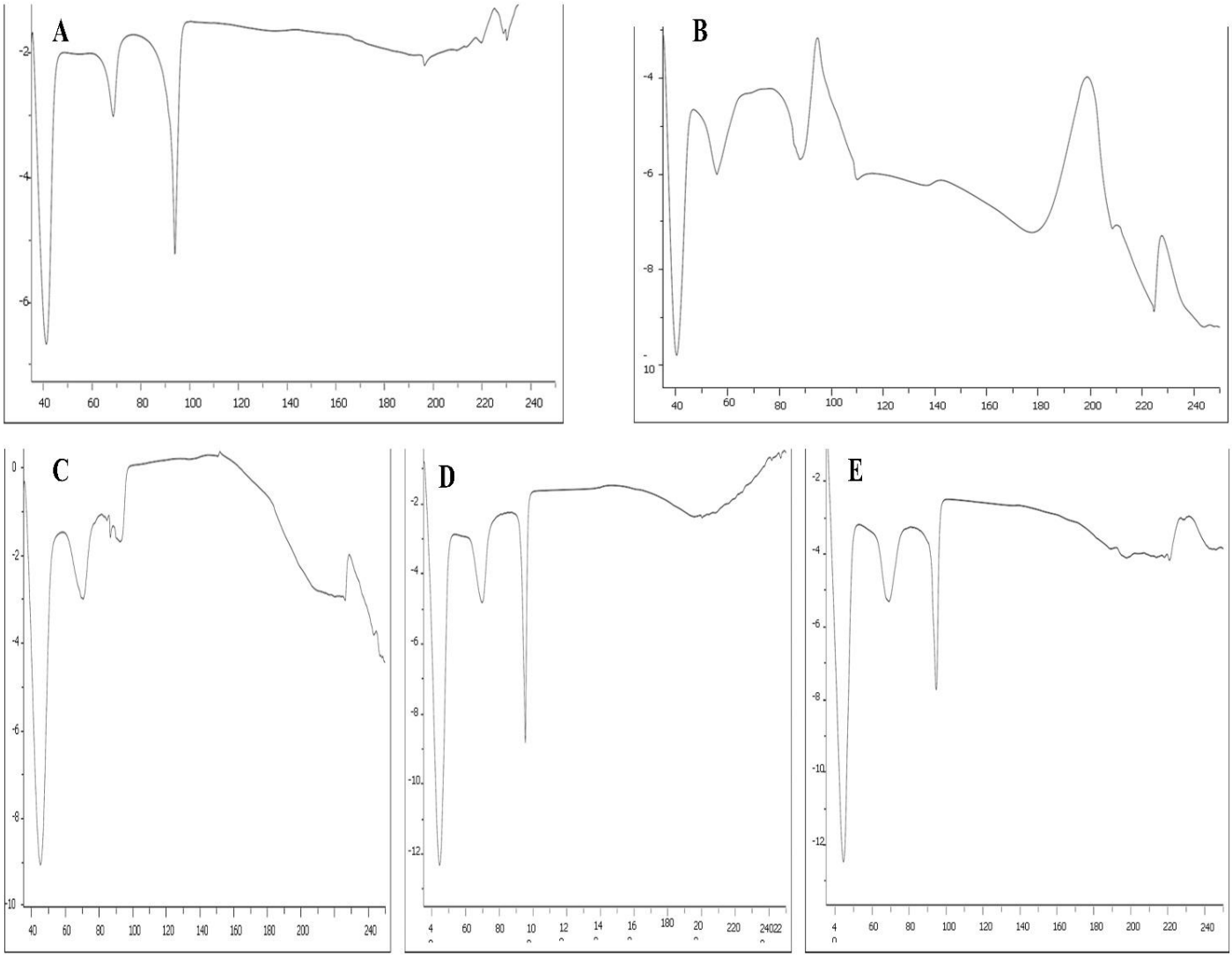

Figure 4: DSC thermogram of curcumin(A), Sodium starch glycolate (B), batch A (C), batch B (D) and batch C (E).

Figure 4 shows DSC thermograms of sodium starch glycolate, curcumin and batches A, B and C. Curcumin exhibited a distinct endothermic peak in the approximate temperature range of 175-185

ºC, consistent with its melting transition and crystalline nature. SSG showed a broad thermal event below 100 °C, which may be associated with the loss of moisture or other thermally induced changes in the hydrophilic polymer.

In the thermograms of batches A, B, and C, the characteristic endothermic peak observed for curcumin was not detected. Batch A exhibited thermal features attributable to the polymer while Batch B showed a broad endothermic event in the approximate range of 50-100 ºC. Batch C exhibited a thermal event at approximately 65.1 °C. The disappearance of the characteristic curcumin endotherm in the formulated batches indicates that the thermal behaviour of curcumin in the formulations differed from that of the pure drug. This observation may be associated with a reduction in detectable crystalline curcumin or changes in the physical state of the drug or interactions during drying.

The release study of curcumin solid dispersions was conducted to determine the percentage release over a 6-hour period for the three batches (A, B, and C). Batch A showed a moderate release profile with a rapid onset of release. Peak release was observed at 2 hours, after which the release plateaued gradually and showed a slight decline. Batch B exhibited a comparatively steady and prolonged release pattern. Maximum drug release occurred between 2 and 3 hours, followed by a gradual decrease. The release remained higher than the other batches during the later hours of the study. Batch C demonstrated a faster but less sustained release, with distinct peaks at 2 and 3 hours and a notable drop thereafter. Across all formulations, peak drug release occurred between 2 and 3 hours after which the release rate declined. However, Batch B maintained the most stable release over an extended period compared to Batches A and C.

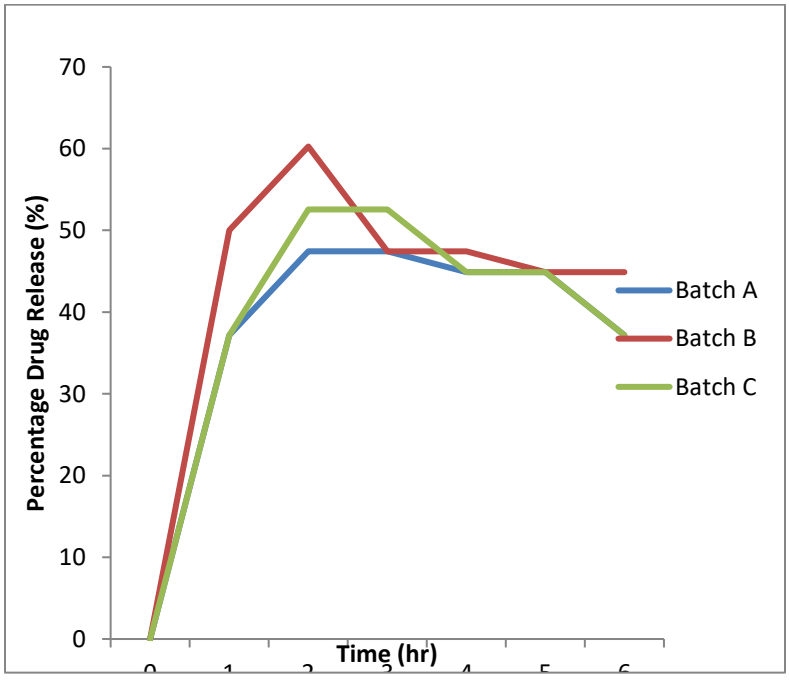

Figure 5: Percentage release (%) of different curcumin solid dispersion (SDC) batches

Batch A (1:1 of curcumin to SSG); Batch B (1:2 of curcumin to SSG); Batch C (2:1 of curcumin to SSG)

Stability studies

The stability study of the three curcumin solid dispersion batches was conducted over a 4-week period, assessing the percentage reduction in drug content during storage (Figure. 6). For Batch A, percentage drug reduction rose markedly from 34.76 % at week 2, to 66.1 % at week 3, reaching 76.26 % at week 4. Batch B demonstrated a similar trend, with percentage reductions of 35.76 % at week 2, 66.79 % at week 3 and 72.86 % at week 4. Batch C showed progressive reductions of 36.34 %, 67.24 %, and 71.82 % at weeks 2, 3, and 4 respectively.

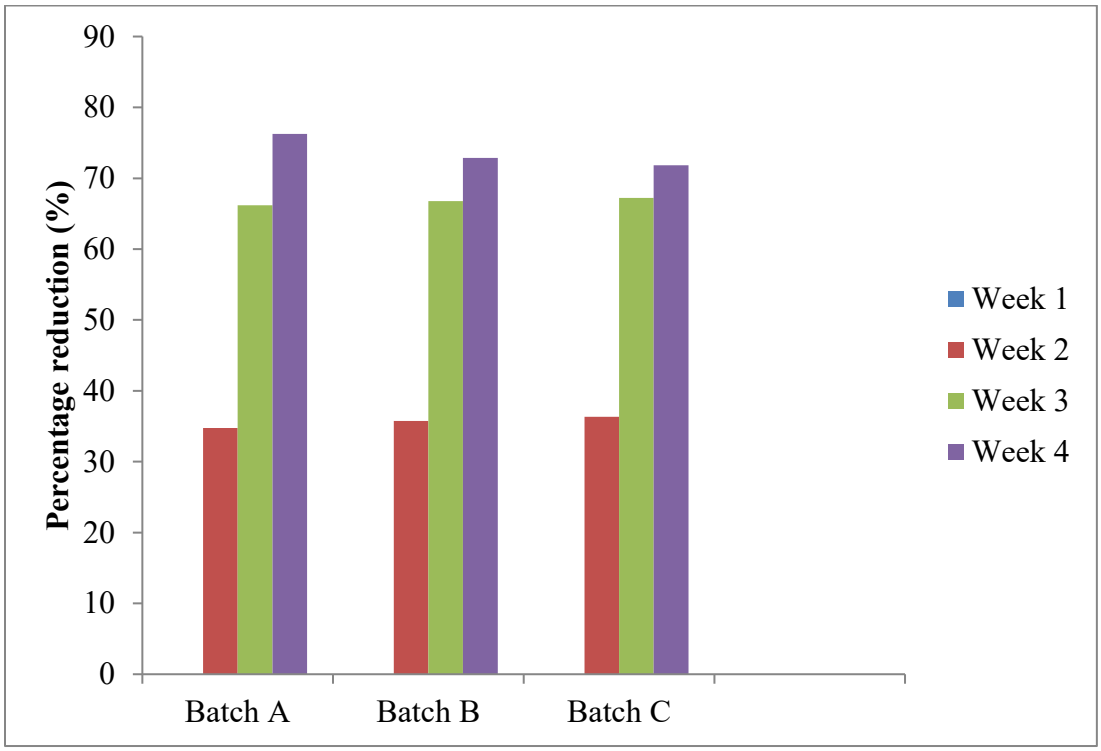

Figure 6: Percentage reduction (%) of different SDC ratios over a period of 4 weeks

Batch A (1:1 of curcumin to SSG); Batch B (1:2 of curcumin to SSG); Batch C (2:1 of curcumin to SSG)

***In vivo* studies of arthritic induced animals**

Limping behaviour was assessed as an indicator of joint inflammation and pain response in arthritic animal models. Animals in the control group (Group 1) showed significant locomotor impairment, with only 28.6 % exhibiting no limping, 57.1 % exhibiting mild limping and 14.3 % showing severe limping. This reflected persistent inflammation in untreated arthritic animals.

Treatment with diclofenac sodium produced a total of 71.4 % of treated animals with no limping, 28.6 % with only mild limping and none displaying severe limping. Among the curcumin solid

dispersion formulations, Group 4 (batch B) demonstrated the highest improvement, with 85.7 % of animals showing no limping and 14.3 % showing mild symptoms. Group 3 (batch A) exhibited moderate improvement, with 57.1 % of animals showing no limping and 42.9 % showing mild limping. Group 5 (batch C) showed improvement similar to Group 4, indicating good therapeutic performance.

Knee swelling was also assessed as a key indicator of inflammation and arthritic progression over a one-month period across five treatment groups. No severe swelling was recorded. Group 3 (batch A) showed a moderately less favourable response, with only 14 % of animals showing no swelling while 86 % continued to show mild swelling. Group 5 (batch C) demonstrated therapeutic performance comparable to Group 4 (Batch B) and diclofenac, showing effective reduction in swelling without any severe swelling cases.

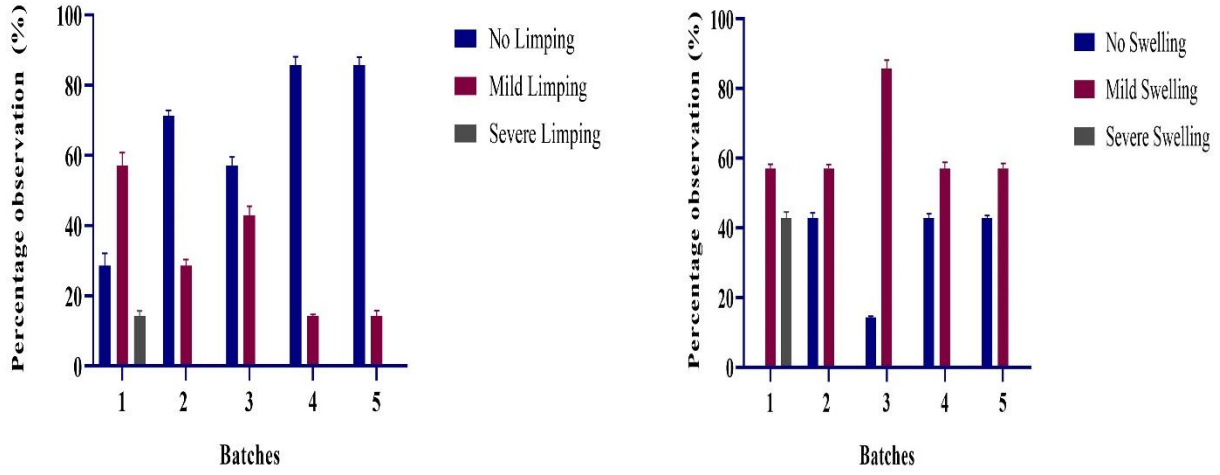

Figure 7: Chart of limping and swelling behaviours (percentage value) for different treatment groups after 28 days

Key: Group 1: distilled water (negative control); Group 2: diclofenac sodium (positive control); Group 3: batch A; Group 4: batch B; Group 5: batch C

In the assessment of the therapeutic efficacy of the curcumin solid dispersions using percentage arthritic inhibition as the primary index, the negative control group consistently showed the lowest inhibition values throughout the study. Arthritic inhibition remained at 0 % from days 4 to 28, indicating progressive joint degeneration in the absence of pharmacological intervention. In contrast, the positive control group (diclofenac-treated) displayed a significant and steady reduction in arthritic symptoms. Inhibition began at approximately 60% on day 4 and increased progressively to 95 % by day 28. Among the curcumin solid dispersions, Group 4 (batch B)

exhibited the highest therapeutic effect. Inhibition increased from approximately 75 % on day 4 to 100 % by day 28, reflecting complete suppression of arthritic symptoms. Group 3 (batch A) demonstrated moderate outcomes. Inhibition began near 40 % on day 4, rising to 75 % by day 28. Although it outperformed the untreated group, it lagged behind both the diclofenac and other SDC formulations. Group 5 (batch C) showed a strong upward improvement, from approximately 60 % on day 4 to over 95% by day 28, comparable to Groups 2 and 3.

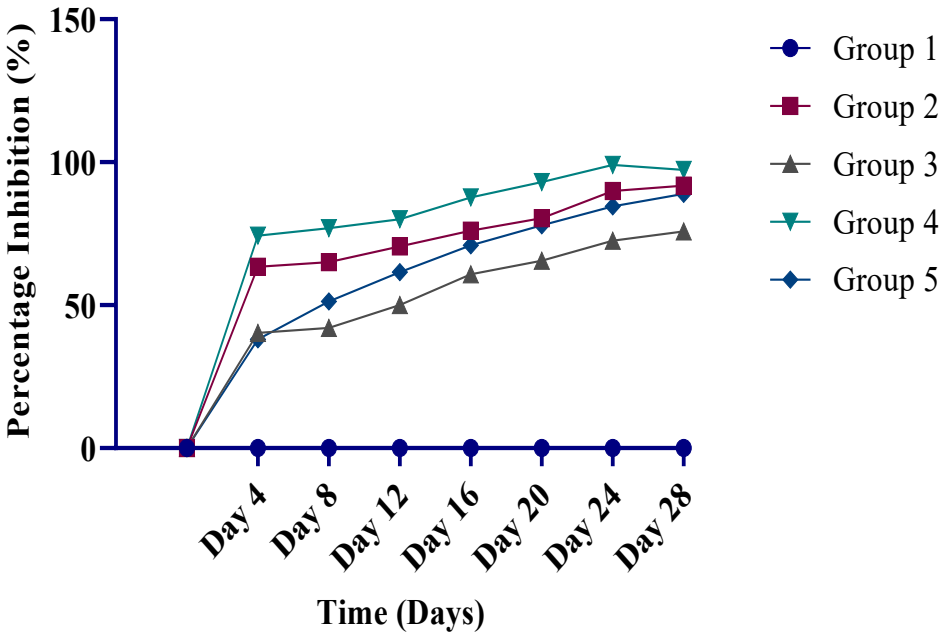

Figure 8: Percentage arthritic inhibition observation in the different treatment groups for 28 days

Key: Group 1: distilled water (negative control); Group 2: diclofenac sodium (positive control); Group 3: batch A; Group 4: batch B; Group 5: batch C

Histological assessment was done using the optimized batch (batch B). The untreated osteoarthritic group exhibited marked alterations in skeletal muscle architecture (Figure 9B), characterized by irregular arrangements, accompanied by inflammatory cell infiltration and increased interstitial connective tissue. In contrast, the curcumin-treated group showed a more organized arrangement of muscle fibres, with compact instertitial spaces and no obvious inflammatory cell infiltration or apparent tissue injury in the examined sections these observations suggest that curcumin treatment was associated with better preservation of skeletal architecture and reduced histological evidence of inflammation and interstitial tissue changes compared with the untreated osteoarthritic group. Muscle fibres appeared disorganized, showing wavy and irregular arrangements rather than the typical parallel alignment characteristic of normal muscle tissue, which the curcumin-treated group showed. Evidence of inflammatory cell infiltration was also observed in the untreated group alongside an increase in interstitial connective tissue, indicating the presence of fibrosis, whereas

the interstitial spaces in the curcumin-treated group appeared compact, with no evidence of injury or inflammatory infiltration (Figure 9A). These features indicate preserved muscle architecture and suggest effective protection of the skeletal muscle tissue in the treatment group.

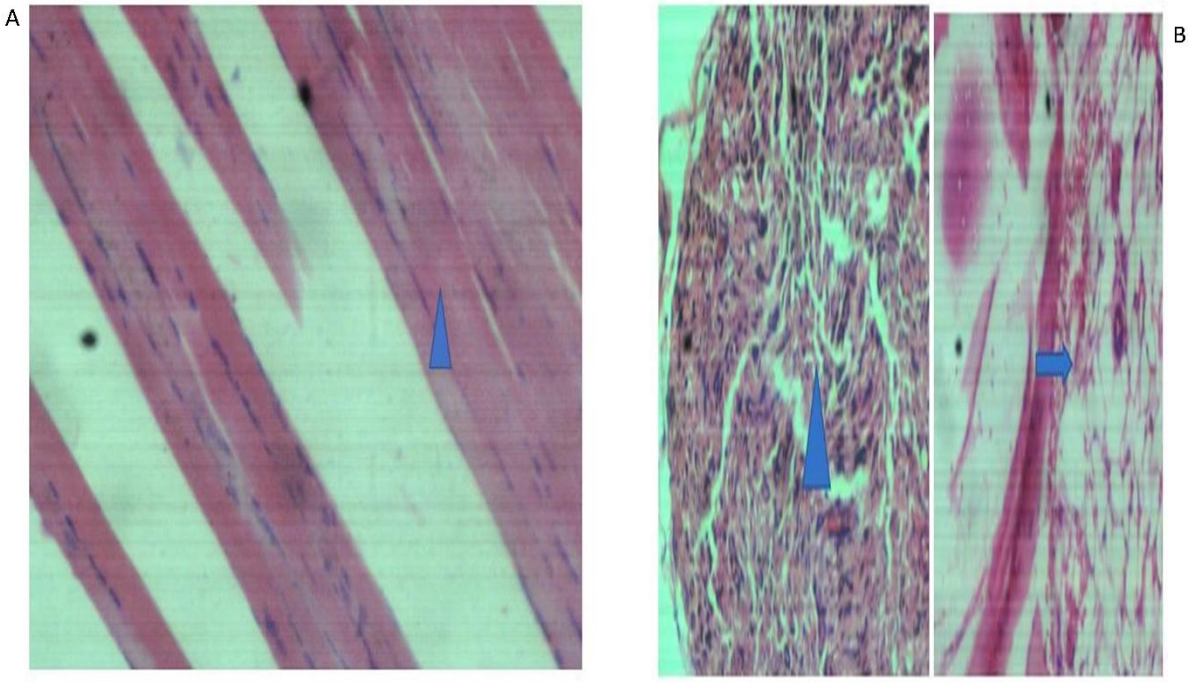

Figure 9: Photomicrograph of knee skeletal muscle tissue section (A= Treated; B= untreated)

Discussion

Dissolution is the rate liming step for less water-soluble medications in their absorption through the oral route. Previous research studies (Nagabandi *et al*., 2014; Hirasawa *et al*., 1998; Kulkarni *et al*., 2012; Akbari *et al*., 2015; Leuner and Dressman, 2000) have demonstrated that the oral absorption and effectiveness of curcumin can be enhanced using manufacturing solid dispersions. In our research, the solid dispersions of curcumin were generated using solvent evaporation system utilizing a hydrophilic carrier, sodium starch glycolate, in different ratios. In the aqueous solubility evaluation, there was a marked improvement in solubility across all solid dispersion batches which confirmed that dispersing curcumin in a hydrophilic polymer matrix enhances its solubilization potential. Increased aqueous solubility observed in batches B and C may be attributed to improved drug dispersion, reduced particle size, enhanced wettability, and potential reduction in crystallinity within the polymer network. Sodium starch glycolate, being a hydrophilic polymer, likely facilitated faster water uptake and matrix hydration, thereby increasing the dissolution rate of curcumin. The superior performance of Batch B supports earlier findings by Patel *et al*., (2021), who demonstrated that higher polymer concentration improves drug-

polymer interactions and molecular dispersion, thereby enhancing aqueous solubility. Meanwhile, the high solubility observed in Batch C despite its increased drug load suggests that the dispersion and hydration dynamics of the matrix were sufficiently optimized. This aligns with the observations of Vasconcelos *et al*. (2016), who reported that solid dispersions can maintain improved solubility at higher drug loads provided crystallinity reduction is achieved and the matrix hydrates rapidly.

For the percentage curcumin release, batch C, which contained a higher proportion of curcumin relative to SSG, exhibited the highest experimental drug content (63.59%). Conversely, batch B, which contained twice as much SSG as curcumin, exhibited the lowest drug content (32.99%). This observation reflects the expected influence of formulation composition on the percentage of drug present in the solid dispersion. The theoretical drug contents calculated from the curcumin-to-sodium starch glycolate ratios were 66.67%, 50.00%, and 33.33% for batches C, A, and B, respectively. Although, the experimental values followed the same ranking as the theoretical values, the measured drug contents were lower than their respective theoretical values in all three batches. The magnitude of these differences varied among the formulations with batch B exhibiting close agreement between theoretical and experimental values, with a difference of only 0.34 percentage points, batch C an intermediate difference of 3.08 percentage points and batch A largest difference of 5.21 percentage points. The relatively close agreement observed for batch B suggests that its measured drug content most closely approximated the theoretical composition among the three formulations. The differences between the theoretical and experimental drug contents may be associated with factors arising during the formulation preparation, sample handling, or analytical determination such as processing losses, incomplete extraction of curcumin from the solid dispersion and analytical variability. (ICH Q2(R2) Guideline,2023)

In our DSC experiment, the absence of the characteristic curcumin melting endotherm suggests that the thermal behaviour and detectable crystalline state of curcumin were altered following formulation with SSG. This observation may indicate a reduction in the amount of crystalline curcumin present in the formulations. The broad thermal event observed for Batch B between approximately 50 and 100 ^{o}C and the event at 65.1 ^{o}C observed for batch C may be associated with moisture-related or other thermal transitions involving the hydrophilic polymer matrix.. Overall, the DSC findings indicate that the thermal characteristics of curcumin changed following formulation with SSG. Although the disappearance of the characteristic melting endotherm is consistent with possible reduction in detectable crystalline curcumin, further solid-state characterization would be required to confirm the extent of amorphization or molecular dispersion in the individual batches (Marano *et al*., 2016).

The FTIR spectra of curcumin, SSG, and their solid dispersion formulations revealed characteristic absorption bands associated with the functional groups of the individual components. The persistence of several

characteristic curcumin bands in batches A, B, and C suggests that these functional groups remained detectable following formulation.

Differences in position, width and intensity of selected absorption bands among the formulations suggest that the incorporation of curcumin into SSG matrix may have altered the local chemical environment of some functional groups. Changes involving O-H stretching bands may be consistent with intermolecular interactions, including hydrogen bonding, between curcumin and the polymer. However, because band shifts and broadening can arise from several factors, including overlapping absorptions and differences in the physical environment, the FTIR results alone do not establish the presence or relative strength of hydrogen bonding in the individual batches. Similarly, the retention of characteristic absorption bands does not exclude changes in the physical state or molecular arrangement of curcumin within the formulations. The observed spectra provide no definitive evidence of new covalent bond formation, although the possibility of non-covalent interactions cannot be conclusively established from FTIR alone. Overall, the FTIR findings are consistent with the incorporation of curcumin into SSG matrix, with possible changes in the local chemical environment of some functional groups.

The dissolution behaviour of Batch A showed an initial rapid release due to sufficient wetting and surface exposure of curcumin, then a subsequent plateau and slight decline. Although the equimolar ratio provided balance, it was not optimal for maintaining higher release over prolonged durations.

Batch B displayed a more sustained and extended-release profile, likely due to its higher polymer content, which enhances drug-polymer interactions, wetting, solubilization, and delays recrystallization. This interpretation aligns with Rajalakshmi *et al*. (2019), who reported that increasing carrier concentration improves amorphization, reduces drug aggregation, and significantly enhances the dissolution rate of poorly soluble drugs. Batch C released curcumin rapidly but could not sustain the release beyond 3 hours. This may be due to insufficient carrier content leading to incomplete dispersion and precipitation of undissolved curcumin. This observation is reported by previous studies by Rao and Prasad (2018), who found that higher drug loading accelerates crystallization and reduces long term solubility and bioavailability. Comparatively, Batch B demonstrated superior prolonged release behavior, suggesting that higher polymer concentrations improve the solubility and sustained dissolution of curcumin. This concurs with findings by Patel *et al.* (2016), who reported that enhanced polymer content increases surface area, wetting, and molecular dispersion, resulting in improved dissolution performance.

The increasing percentage reduction of curcumin across all batches confirms that curcumin degrades progressively during storage, consistent with the known sensitivity of curcumin to environmental stressors such as moisture, oxygen and temperature. However, the relatively lower degradation

observed in Batch B indicates that formulation with higher polymer-to-drug ratio (1:2) may improve stability. These findings align with previous studies on the stability of curcumin solid dispersions. Hazra *et al*. (2015) and Ireson *et al*. (2001) reported that polymeric carriers such as PVP and cellulose derivatives improve both solubility and chemical stability of curcumin by forming stronger intermolecular interactions and helping maintain the amorphous state of the drug. Similarly, Tran *et al*. (2019) found that dispersions containing higher polymer concentrations demonstrated superior storage stability under accelerated conditions. The enhanced stability in Batch B may be attributed to the greater availability of hydrophilic carrier, which can form additional hydrogen bonds with curcumin, restrict molecular motion, and create a microenvironment that minimizes exposure to degradation triggers such as moisture and oxygen. This agrees with the general principles of solid dispersion technology, which state that increasing carrier content often reduces degradation rates (Patel *et al*., 2021). Overall, the results suggest that the 1:2 polymer-to-drug ratio (Batch B) provides the most favourable stability profile, making it the most suitable formulation for maintaining curcumin integrity during storage.

Among the curcumin solid dispersions, the superior improvement in locomotor performance observed in Group 4 (batch B) suggests enhanced bioavailability at this drug-to-polymer ratio. This is consistent with findings by Patel *et al*. (2021), who noted that hydrophilic polymer carriers improve curcumin dissolution and absorption, thereby enhancing therapeutic outcomes. The moderate improvement in Group 3 (batch A) may indicate limited dispersion efficiency at this ratio, potentially reducing curcumin release and absorption. This highlights the importance of optimizing polymer concentration for effective solid dispersion performance. The strong response in Group 5 (batch C) is supported by studies by Rahman *et al.* (2022), which showed that formulations with increased curcumin content can maintain or enhance anti-inflammatory potential up to a certain threshold. Again, the strong response in reducing swelling seen in SDC with batch B (Group 4) reflects improved curcumin performance when delivered via solid dispersion. This corresponds with studies by Patel *et al.* (2021), which attribute enhanced anti-inflammatory activity to improved solubility, dissolution, and systemic availability of curcumin in polymer-based dispersions. The SDC with batch A (Group 3) gave a comparatively weaker response which could suggest that the 1:1 ratio may limit curcumin release or absorption, reducing therapeutic efficiency. Although no severe swelling was observed, the reduced number of animals with complete swelling resolution indicates suboptimal dispersion at this ratio. Batch C solid dispersion (Group 5) produced improvements in swelling resolution, indicating that curcumin-rich dispersions can maintain substantial anti-inflammatory efficacy. This agrees with findings by Song *et al*. (2016), which highlight the role of increased surface area and enhanced permeability in improving curcumin activity within solid dispersion systems. The

enhanced efficacy can be attributed to improved dissolution properties and increased molecular dispersion of curcumin in these formulations.

For the percentage arthritic inhibition, the poor inhibition observed in the negative control group aligns with earlier findings by Bendele (2001), who reported persistent inflammation and cartilage erosion in MIA-induced OA when no treatment is administered. Then the superior therapeutic performance of batch B (Group 4) suggests enhanced bioavailability and sustained release of curcumin at this polymer-to-drug ratio. This function is buttressed by a previous study which reported that hydrophilic solid dispersion matrices markedly enhance dissolution, absorption, and anti-inflammatory activity of curcumin. (Patel *et al*., 2021). The moderate performance of batch A (Group 3) indicates that this ratio may provide suboptimal curcumin dispersion, resulting in reduced systemic availability. Batch C (Group 5) showed performance comparable to the batch B, suggesting that both curcumin-rich (batch C) and polymer-rich (batch B) solid dispersions can achieve good anti-osteoarthritic activity. A previous study by Rahman *et al*., (2022) actually agrees with this point where optimized curcumin solid dispersions were observed to outperform raw curcumin in reducing joint inflammation. These findings indicate that curcumin solid dispersions especially batch B with 1:2 ratio provide comparable superior arthritic inhibition relative to other ratios. Its enhanced activity likely stems from improved dissolution, enhanced mucosal absorption, and efficient systemic delivery, as supported by Aggarwal and Harikumar (2009).

Furthermore, the histological findings revealed differences in skeletal muscle architecture between the untreated osteoarthritic group and the curcumin-treated group. The disorganized muscle fibres, inflammatory cell infiltration, and increased interstitial connective tissue observed in the untreated group suggest the presence of tissue alterations associated with the experimental conditions (Choudhury *et al*., 2014). Conversely, the more organized muscle fibre arrangement and reduced apparent inflammatory changes in the curcumin-treated group suggest a possible beneficial effect of curcumin on skeletal muscle tissue integrity (Mobasheri *et al*, 2019). These observations may be relevant to understanding the potential effects of curcumin on tissues associated with osteoarthritic condition. However, the histological assessment was limited to skeletal muscle tissue, and the observed changes cannot be used as direct evidence of articular cartilage protection. Further assessment of joint tissues, including articular cartilage and subchondral bone, would be necessary to determine whether curcumin exerts structural protective effects on the osteorthritic joint.

Conclusion

Batch B (SDC ratio 1:2) had the best properties combining optimal flow properties, high solubility, superior release, and greater pharmacological activity.

Acknowledgment: The authors sincerely acknowledge Mr Chibueze Ikeh for assisting with the animal studies of this work.

Ethics approval: All animal experiments were conducted in compliance with National Institute of Health Guidelines for the Care and Use of Laboratory Animals (National Institute of Health (NIH) (2011) (Pub No. 85 - 23). Ethical clearance was also obtained from the Animal Research Ethics Committee (AREC) at Nnamdi Azikiwe University, Anambra State, Nigeria, with the approval number, NAU/AREC/2025/0184.

Competing interests: The authors declare no competing interests in this work.

Funding information: The authors state no funding received for this work,

Authors contributions: Onwunedo Afomachukwu Chinelo: Conceptualization, Methodology, Investigation, Data Curation, Data interpretation, Writing-original draft preparation; Modozie Benjamin Uchenna: Investigation, analysis; Emmanuel Uronnachi: Supervision, Validation, Reviewing, Editing.

Data availability statement: The datasets generated and/or analyzed during the current study have been included in the work. Any additional information is available from the corresponding author on reasonable request.

References

Aggarwal, BB, & Harikumar, KB. (2009): Potential therapeutic effects of curcumin, the anti-inflammatory agent, against neurodegenerative, cardiovascular, pulmonary, metabolic, autoimmune and neoplastic diseases. The International Journal of Biochemistry & Cell Biology, 41(1), 40-59. http://doi.org/10.1016/j.biocel.2008.06.010

Akbari J, Enayatifard R, Saeedi M, Morteza-Semnani K, Rajabi S. (2015): Preparation, characterization, and dissolution studies of naproxen solid dispersions using polyethylene glycol 6000 and labrafil M2130, Pharm. Bio. Res. 1 (2) 44–53.

Bendele, AM. (2001): Animal models of osteoarthritis. Journal of Musculoskeletal & Neuronal Interactions, 1(4), 363–376

Chen X, McClements DJ, Zhu Y, Chen Y, Zou L, Liu W, Cheng C, Fu D, Liu C. (2018): Enhancement of the solubility, stability and bioaccessibility of quercetin using protein-based excipient emulsions. Food Res. Int.114:30–37. doi: 10.1016/j.foodres.2018.07.062.

Choi, JS, Lee, SE, Jang, WS, Byeon, JC, Park, JS. (2018): Solid dispersion of dutasteride using the solvent evaporation method: Approaches to improve dissolution rate and oral bioavailability in rats. Materials Science and Engineering: C,90, 387-396. doi:10.1016/j.msec.2018.04.074.

Choudhury ST, Das N, Ghosh S, Ghosh D, Chakraborty S, Ali N. (2016). Vesicular (liposomal and nanoparticulated) delivery of curcumin: A comparative study on carbon tetrachloride-mediated oxidative hepatocellular damage in rat model. Int. J. Nanomed. 11:2179–2193. doi: 10.2147/ijn.s101886.

Franco M, Trapani G, Latrofa A, Tullio C, Provenzano MR, Serra M, Liso G. (2001): Dissolution properties and anticonvulsant activity of phenytoin-polyethylene glycol 6000 and-polyvinylpyrrolidone K-30 solid dispersions, Int. J. Pharm. 225 (1–2) 63–73.

Fu XY, Yang MF, Cao MZ. (2016). Strategy to suppress oxidative damage-induced neurotoxicity in PC12 cells by curcumin: the role of ROS-mediated DNA damage and the MAPK and AKT pathways. Mol Neurobiol. 53(1):369–378.

Gohel MC, Patel LD. (2003). Studies on formulation of nimesulide-SSG dispersible tablets. Drug Dev Ind Pharm.29(8):927-934.

Guzman RE, Evans MG, Bove S, Morenko B, Kilgore K. (2003). Mono-iodoacetate-induced histologic changes in subchondal bone and articula cartilage of rat femorotibial joints: An animal model of osteoarthritis. Journal of Toxicologic Pathology. Doi: 10.1080/01926230390241800

Hazra M, Mandal DD, & Mandal T. (2015). Solubility enhancement of curcumin via solid dispersion technology: A comprehensive review. International Journal of Pharmaceutical Sciences and Research, 6(2), 443-456.

Hernandez M, Wicz S, Corral RS. (2016). Cardioprotective actions of curcumin on the pathogenic NFAT/COX-2/prostaglandin E-2 pathway induced during Trypanosoma cruzi infection. Phytomedicine. 23:1392–1400.
doi: 10.1016/j.phymed.2016.06.017.

Hirasawa N, Danjo K, Haruna M, Otsuka A. (1998) Physicochemical characterization and drug release studies of naproxen solid dispersions using lactose as a carrier, Chem. Pharm. Bull. 46 (6) 1027–1030, https://doi.org/10.1248/cpb.46.1027.

Ireson C, Orr S, Jones DJL, Verschoyle R, Lim CK, Luo JL, Howells L, Plummer S, Jukes R, Williams M. (2001): Characterization of metabolites of the chemopreventive agent curcumin in human and rat hepatocytes and in the rat in vivo, and evaluation of their ability to inhibit phorbol ester-induced prostaglandin E2 production. Cancer Res. 61:1058–1064.

Kulkarni A, Bhatia M, Rathore D. (2010). DSC and XRD studies of sodium starch glycolate and crospovidone. J Pharm Res.3(5):1085-1089

Kulkarni PK, Dixit M, Panner S, Achin J. (2012) Preparation and evaluation of naproxen solid Dispersion Technique, Int. Res. J. Pharm. 3 174–177.

Leuner C, Dressman J. (2000) Improving drug solubility for oral delivery using solid dispersions, Eur. J. Pharm. Biopharm. 50 (1) 47–60.

Liu FR, Gao S, Yang YX, Zhao XD, Fan YM, Ma WX, Yang DR, Yang AM, Yu Y. (2018). Antitumor activity of curcumin by modulation of apoptosis and autophagy in human lung cancer A549 cells through inhibiting PI3K/Akt/mTOR pathway. Oncol. Rep. 39:1523–1531.
doi: 10.3892/or.2018.6188.

Lukulay P, Hokanson G. (2005). Reconciling mass balance in forced degradation studies. Pharmaceutical Technology, 29 (10).

Marano S, Barker SA, Raimi-Abraham BT, Missaghi S, Rajabi-Siahboomi A, Craig DQ.

(2016): Development of micro-fibrous solid dispersions of poorly water-soluble drugs in sucrose using temperature-controlled centrifugal spinning, Eur. J. Pharm. Biopharm. 103 84–94, https://doi.org/10.1016/j. ejpb.2016.03.021

Meng B, Li J, Cao H. (2013): Antioxidant and antiinflammatory activities of curcumin on diabetes mellitus and its complications. Curr. Pharm. Des. 19:2101–2113.

Mobasheri A, Priem F, Henrotin Y. (2019). Curcumin and osteoarthritis: therapeutic potential and molecular targets.Drugs in context, 8,212574

Mohammadia M, Salami M, Momen S, Alavi F, Emam-Djomeh Z, Moosavi-Movahedi AA (2019). Enhancing the aqueous solubility of curcumin at acidic condition through the complexation with whey protein nanofibrils. Food Hydrocoll.87:902–914. doi: 10.1016/j.foodhyd.2018.09.001.

Nabavi SF., Daglia M, Moghaddam AH, Habtemariam S, Nabavi SM. (2014). Curcumin and liver disease: From chemistry to medicine. Compr. Rev. Food Sci. Food Saf. 13:62–77. doi: 10.1111/1541-4337.12047.

Nagabandi V, Chandragiri AK, Thota S, Katakam P. (2014) Enhancement of dissolution rate of naproxen by lipid based solid dispersions, J. Pharmaceut. Sci. Res. 6 (2)78.

Nicoliche T, Maldonado DC, Faber J, Pereira da Silva MC. (2020) Evaluation of the articular cartilage in the knees of rats with induced arthritis treated with curcumin. PLOSONE, 15(3), E0230228.

Pari, L, Tewas, D. Eckel, J. (2008) Role of curcumin in health and disease. Archives of Physiology and Biochemistry. 2008;114(2):127-149

Patel RP, Patel MM, Patel NM. (2016). Study of solid dispersion technique for dissolution enhancement of poorly water-soluble drug. Journal of Pharmacy Research, 9(6), 69-475.

Patel, AR, Velikov, KP, Goycoolea, FM. (2021). Colloidal delivery systems in the development of curcumin as a therapeutic: Challenges and opportunities. ACS Nano, 15(3), 4541–4557.

Pitcher T, Sousa-Valente J, Malcangio M. (2016). The monoiodoacetate model of osteoarthritis pain in the mouse. Journal of Visualized Experiments, (111), 53746. doi:10.3791/53746

Rahman MM, Islam MS, Uddin, MB. (2022). Enhancement of curcumin bioavailability using solid dispersion technique: Formulation optimization and evaluation. Journal of Drug Delivery Science and Technology, 67, 102984.

Rajalakshmi G, Kumar S, Senthilkumar N (2019). Dissolution enhancement of curcumin using hydrophilic carriers by solid dispersion technique. Journal of Drug Delivery and Therapeutics, 9(4), 427-432.

Rao M, Prasad D. (2018). Effect of drug: plymer ratio on physical stability and solubility of curcumin solid dispersions. Asian Journal of Pharmaceutics, 12(3), 789-795.

Reggane M, Wiest J, Saedtler M, Harlacher C, Gutmann M, Zottnick SH, Piechon P, Dix I, Müller-Buschbaum K, Holzgrabe U. (2018). Bioinspired co-crystals of imatinib providing enhanced kinetic solubility. Eur. J. Pharm. Biopharm.128:290–299. doi: 10.1016/j.ejpb.2018.05.012.

Seo B, Kim T, Park HJ, Kim JY, Lee K.D, Lee JM, Lee YW. (2016). Extension of the hansen solubility parameter concept to the micronization of cyclotrimethylenetrinitramine crystals by supercritical anti-solvent process. J. Supercrit. Fluids.111:112–120. doi: 10.1016/j.supflu.2016.01.015.

Shihora H, Panda S. (2011). Superdisintegrants, Utility in dosage forms: a quick review, J. Pharm.Sci. Bio. Res. 1 (3) 148–153.

Song IS, Cha JS, Choi MK. (2016). Characterization, in vivo and in vitro evaluation of solid dispersion of curcumin containing d-α-tocopheryl polyethylene glycol 1000 succinate and mannitol. Molecules,21(10), 1386.

Tran P, Pyo YC, Kim DH, Lee SE, Kim JK, Park JS. (2019). Overview of the manufacturing methods of solid dispersion technology for improving the solubility of poorly water-soluble drugs and application to anticancer drugs. Pharmaceutics, 11(3), 132.

Vasconcelos T, Sarmento B, Costa P. (2016). Solid dispersions as strategy to improve oral bioavailability of poorly water-soluble drugs. Drug Discovery Today, 21(7), 1063–1078.

Verheyen,S, Blaton N, Kinget R, Mooter GV. (2002). Mechanism of increased dissolution of diazepam and temazepam from polyethylene glycol 6000 solid dispersions, Int. J. Pharm. 249 (1–2) 45–58.

Wong JJL, Yu H, Lim LM, Hadinoto K. (2018). A trade-off between solubility enhancement and physical stability upon simultaneous amorphization and nanonization of curcumin in comparison to amorphization alone. Eur. J. Pharm. Sci.114:356–363. doi: 10.1016/j.ejps.2018.01.010.

Xu W, Sun Y, Du L, Chistyachenko YS, Dushkin AV, Su W. (2018). Investigations on solid dispersions of valsartan with alkalizing agents: Preparation, characterization and physicochemical properties. J. Drug Deliv. Sci. Technol.44:399–405. doi: 10.1016/j.jddst.2018.01.012

Yadav JN, Tekade AR. (2020): A review on solid dispersion and carriers used therein for solubility enhacement of poorly water-soluble drugs. Advanced Pharmaceutical Bulletin, 10(3), 359-369.

Yu JY, Kim JA, Joung HJ, Ko JA, Park HJ. (2020): Preparation and characterization of curcumin solid dispersions using HPMC. J Food Sci. 85(11): 3866-3873.doi:10.1111/1750-3841.15489.